



MAPPING KARST FEATURES

Testing a Method to Map the Abundant Karst Features within
Logan Canyon

“Logan Canyon with its alpine wildflowers, limestone cliffs, rushing trout streams, and myriad other signatures of nature upon unsullied canvas – remains something to be treasured and preserved.”

~Michael S. Sweeny~

Dane Brophy
Undergraduate Researcher
Hydrogeology Major, GIS Minor
Utah State University
CEE 6440

Abstract

Through quantifying and comparing spectral signatures, thermal anomalies, and watersheds within areas of known surface karst features (caves and sink holes), this study determines that there are patterns that can be used to assist in identifying locations where unmapped features exist.

Introduction

This study hypothesizes that remote sensing can provide a method for detecting previously unmapped openings into karst systems. Previous studies have produced a lot of knowledge about Logan Canyon hydrology, including that the karst networks and their effects on water is incredibly complex. Nonetheless, they also show that there is still much to learn if an understanding of the subsurface drainages is to be reached. The importance of comprehending the workings of the karst features in the canyon is due to reliance on the water that it transports to surrounding communities. Water from the Logan River generates electricity and further irrigates agricultural and urban areas. Moreover, the karst networks and aquifers also provide drinking water to surrounding areas. Finally, the river also directly maintains environmental integrity, habitat, and the bounty of recreational areas throughout Cache Valley.

Further benefits to an increased understanding of the complexity of karst features are easily identifiable based on what we know about similar karst networks. When comparing volumes of water in karst aquifers to waterways on the surface, karst aquifers receive more recharge, and both store and transmit larger volumes of water (Kresic, 2013). Therefore, it becomes clear that an improved understanding of underground reservoirs and rivers within karst features would result in a better understanding of our groundwater stores and determine how the anticipated shift from a snow-dominated system to a rain-dominated system will affect our water resources.

Before a better understanding of the inaccessible conduits and subsurface connections can be gained, a larger percentage of surface karst features must be mapped. Towards that end, this research will provide insight into the type and location of surface karst features in relation to the geology and structure of Logan Canyon.

Previous Work

Spangler (2011) used dye tracing to measure flow-through rates of the karst drainages and mapped the pour points of some of the larger karst features within Logan Canyon. Additionally, through chemical signatures of the ground water, he was able to suggest that the rocks through which the conduits run have notable differences. Bahr (2016) focused on mapping the karst features in the locale of Tony Grove to study how structures within the geology affected the karst complexes. Bahr showed

that these alpine karst systems are “highly influenced” by the orientation, geometry, permeability, and deformation of the rock units in which they are located.

A statewide, multi-university, NSF funded project, iUtah, has put an emphasis on measuring and documenting many hydrologic factors that affect the Logan River, as well as direct measurements of water quality parameters. Data resulting from this project provides the basis for many pertinent questions about how climate change, and the anticipated warmer air temperatures, will alter snowpack accumulation and snowmelt. More importantly to the local community, this has led to questions regarding the connections to groundwater recharge and changes to river and spring discharge throughout the watershed (Neilson et al. 2018).

A recent three-year study used water chemistry, discharge measurements, and other information to show that there is a substantial link between snowmelt, karst drainage, baseflow, and discharge variations in the Logan River (Neilson et al. 2018). Additionally, this study documented large gains and losses of water volume over expanses of the river’s channel. Supplementary historical data analysis has further related maximum snow water equivalent to baseflow in the river where the karst terrain plays a major role in water delivery to the river throughout the year.

Study Area

The study area for this project is in Logan Canyon approximately 20–25 km. east–northeast of the City of Logan in the local of a recreational area known as Tony Grove (Fig. 1). Logan Canyon is located in northern Utah’s Bear River Range and is the consequence of a complex geologic history. Nonetheless, for the sake of this paper only a brief geologic history will be given.

The first hints of what is visible in the Bear River Range occurred with shoreline deposition from the Paleozoic Era through the Cambrian Period. This deposition is evidenced by the formations comprising Logan Canyon, which are primarily carbonates and quartz-cemented quartz sandstone (Williams, 1962). Following deposition, Cretaceous west-to-east thrusting occurred during the Laramide Orogeny. That mountain building event resulted in the folding and faulting of rocks. Finally, Basin and Range extension occurred during the Miocene Epoch. This formed the horst-graben structure that juxtaposes Cache Valley and the Bear River Range today (Janecke and Evans, 1999).

One of the prominent features within Bear River Range formations is an incredible amount of karst features, such as sinkholes and cave structures, which act as subsurface drainage networks (Spangler, 2011) (Fig. 2). These karst aquifers are primarily located at higher elevations where there is an abundance of precipitation in the form of snow (Spangler, 2011). Carbonates within the Bear River Range tend to act as water conduits. Within those carbonates water flows through fractures, along

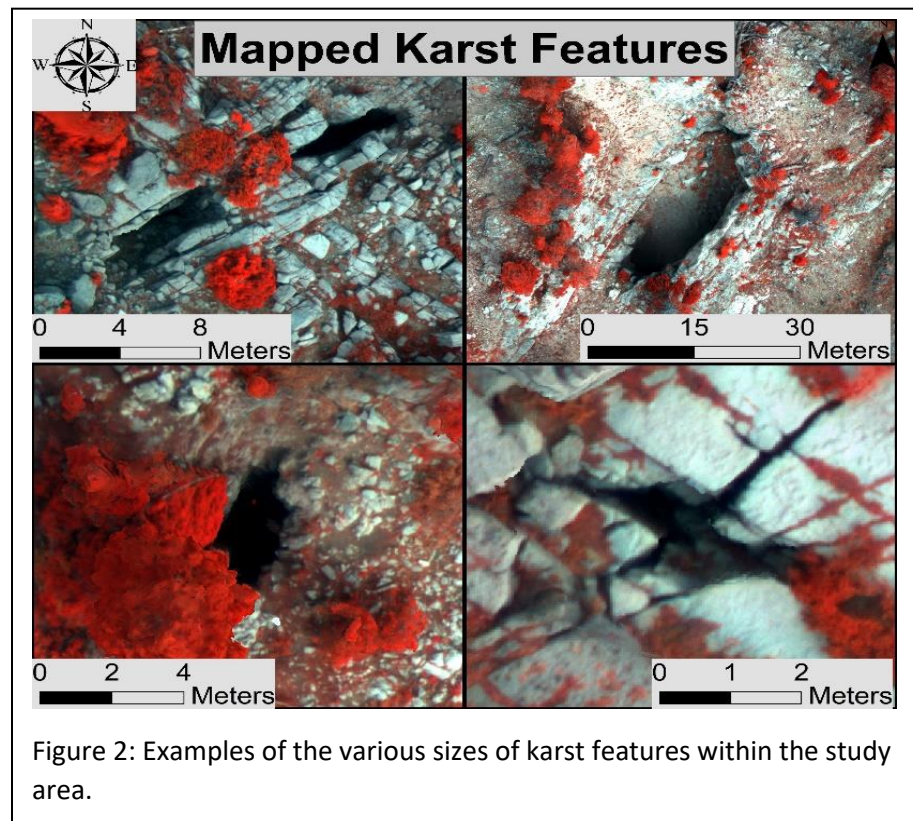
bedding planes, and continually develops dissolution features (Spangler, 2011). Quartzite within the canyon typically acts as a barrier and confines much of the conduit formations to the upper portion of the regional Logan Peak syncline (Spangler, 2011) (Williams, 1948). While these subsurface channels are known to cross through mountain ranges, many of these conduits

drain to the Logan River (Spangler, 2011). The Logan River drains the Logan Canyon watershed and is a third-order river that flows west-southwest with a snow-melt-dominated hydrograph (Neilson et al. 2018).

Methods

As previously stated, the hypothesis behind this study is that remote sensing can provide a method for detecting previously unmapped openings into karst systems. To test that hypothesis, the common knowledge that subsurface voids retain a relatively stable temperature year-round was exploited. Additionally, the assumption has been made that air exchange occurs between karst features and the surrounding environment. Because previous research has noted that karsting acts as conduits for subsurface water, it is also postulated there should be a detectable watershed which drains to each feature.

Therefore, initial exploration began with obtaining coordinates of studied karst features. That data was used to define a study area and identify a location where two remote stations should be deployed. The data loggers (CR-800) were each programmed to run a sensor (HC2S3-L) to record temperature (temp.) and relative humidity (RH). Readings were taken from the HC2S3-L every 10 seconds and then averaged once every 15 minutes. The remote stations were initially deployed at the location of an iUtah weather station in Cache Valley. This was done as a trial run and to verify



functionality. Following that test, the two stations were then deployed at one of the known karst features within the study area. One station was deployed with the purpose of obtaining temp. and RH near a karst opening. That station was deployed approximately one meter of the opening (Fig. 3). The second station had the purpose of recording data from the area surrounding the karst feature. That station was deployed at an elevation approximately 2 meters below the first and within 20 meters of the karst opening.

Based on that information, a UAV survey was conducted with the purpose of collecting red, green, blue, and near infrared bands; as well as thermal and elevation data. That data was then processed to produce fine resolution Red, Green, Blue (RGB); Near Infrared (NIR), and Thermal (TIR) imagery; as well as a Digital Elevation Model (DEM) in the form of a Digital Surface Model (DSM) (Fig. 4).

Using the resulting, fine-resolution rasters, common characteristics of the study area's karst features were identified within reflectance values, thermal imager, and watersheds. The ranges of that data were recorded and used to as filters to map locations with similar attributes. Finally, results were produced by layering the mapped characteristics and keeping only locations that were common amongst all three files.

Results

Initial work for this project began with obtaining coordinates for known karst features. Because, the Federal Government prohibits that data from being shared publicly, it was only obtained by the Researcher after agreeing to non-disclosure of site locations. Therefore, the coordinates for the karst features will not be produced as part of this report. Once those coordinates were mapped with approximate locations, descriptions of the features were used to select locations for onsite visits. The combination of observations from those visits, and guidance from Dr. David Liddell, a Geologist at Utah State University, were used to select the location to deploy the remote stations.



Figure 3: One of the remote stations deployed to identify differences in temp. and RH between karst features and the surrounding areas.

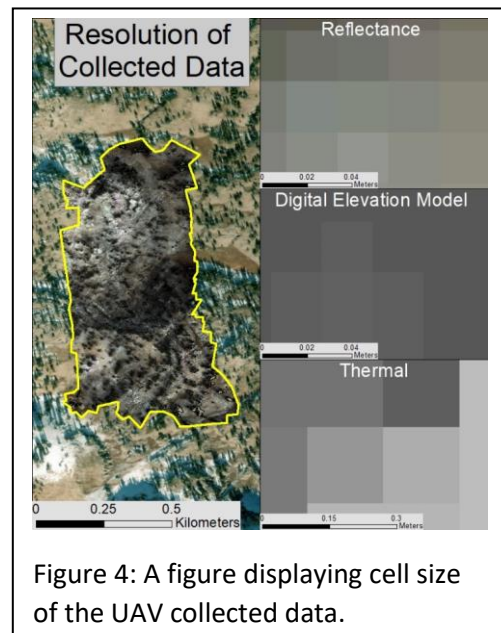



Figure 4: A figure displaying cell size of the UAV collected data.

The remote stations were deployed at a mapped karst feature known as Main Drain on 8/24/18. After a little less than a month's worth of data was recorded, the results were collected on 9/16/18. Expectedly, the resulting data showed that RH was typically higher near the cave. However, contrary to expectations the temp. recorded near the karst feature was typically higher than that of the surrounding area. Data also showed that the greatest difference in temp. and RH during deployment of the remote stations occurred between 9:00 AM and noon (Fig. 5). Therefore, on 9/29/18 the area was surveyed between those hours.

Though initial plans for the drone flight were to use a fixed wing aircraft, the Forest Service wouldn't issue a permit for that type of UAV. Therefore, an octocopter known as Matrice was used to carry out the aerial survey (Fig. 5). However, because Matrice is not capable of surveying as large of an extent as a fixed winged drone, the size of the study site was drastically reduced.

The data which resulted from the aerial survey underwent processing, geolocating, and individual images were stitched together to create a mosaic. However, in the case of the thermal imagery there was an issue with the data that needed to be addressed beforehand. For the drone to reach the study area from the launching point, it had to fly over Tony Grove Lake. Because the air above the lake is much cooler than the surrounding areas, it cooled the thermal sensor. Upon reaching the study area, the sensor then warmed over the duration of the flight as it reacclimated to the surrounding temperatures. Because the thermal sensor is by definition temperature sensitive, the data displayed a gradual change in temperature over the course of the flight path (Fig 6).

To correct the issue, MATLAB was used to plot the minimum and maximum values obtained from each individual image taken over the duration of the survey. Various correction factors were then applied to the data; following which, the results were examined by hand (Fig. 7). A correction factor was found that appeared to correct the issue and was applied to the thermal data. Nonetheless, the Researcher is still mindful of the fact that recorded temperatures may yet be off from actual



UAV:	Matrice 600 Pro
Coverage Area:	0.75 mi^2
Range:	4 mi
Airtime:	30 min
Payload:	5 lbs
Max Weight	32 lbs
Frame Size:	600 mm
Sensors:	Resolution:
RGB-NIR	2 cm
Thermal	15 cm

Figure 5: Specifics of the UAV and its payload sensors used to obtain a fine resolution DEM (Utah State University, 2018).

temperatures. Despite that uncertainty, TIR data was used under the premise that features from the study area had temperatures that correct relative to each other.

In the end, the UAV succeeded in collecting data that resulted in raster layers with a resolution of approximately 2 cm per pixel for the the RGB and NIR imagery, as well as for the DEM. The TIR layer contains a slightly coarser resolution at roughly 15 cm per pixel. The layers were finished being processed and ready for geospatial analysis on 10/27/18.

Work on this project initially used data without concern for the presence of vegetation. However, once the Researcher began working with the DSM, the decision was made to identify a method to remove vegetation and start over. That decision was made after witnessing that hydrologic analysis of the rasters appeared to be influenced by the presence of large trees. Additionally, because imagery-based data lacks usable data from beneath canopies, no possibility existed for analysis of potential karst features located in those shrouded positions.

To successfully remove vegetation, two options were available. The first was to use Agisoft to isolate and remove vegetation through altering variables that defined maximum allowable slope and cell size. However, because the study area contains terrain that is quite steep, it took multiple attempts to differentiate desirable terrain from vegetation (Fig. 8). That posed a problem because the software takes about a day to complete each attempt. Therefore, the Researcher decided to rather use reflectance properties of vegetation to isolate undesirable data.

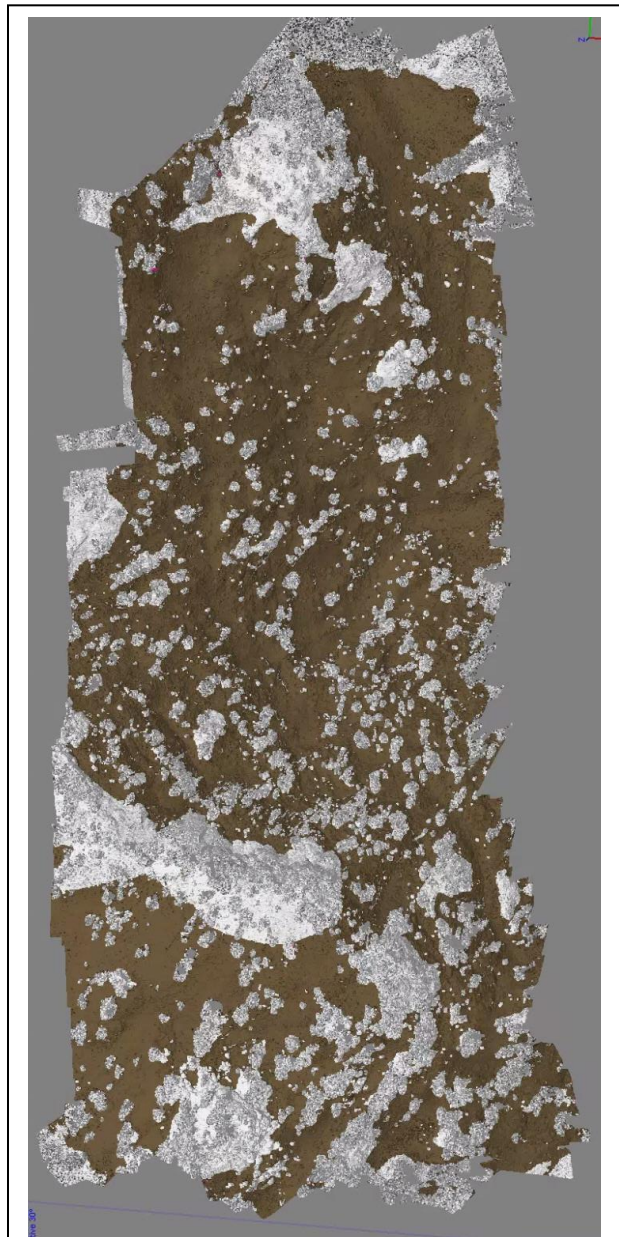


Figure 8: The results from an attempt at removing trees through Agisoft software. White and gray areas are areas where data was removed. Notice no data areas include large sections of terrain.

Under the epidermis of a leaf, there are two primary layers of cells. The upper layer of a leaf is called the palisade parenchyma and is where the majority of chlorophyll is located. When light encounters chlorophyll, typically 60 to 85 percent of the visible wavelengths are absorbed. Of the light that is reflected, it is green light that is reflected strongest. Conversely, NIR wavelengths are affected minimally by the cells within the palisade parenchyma. Rather, NIR wavelengths penetrate through those cells to the second layer called the spongy parenchyma. Cells within this lower layer aren't "packed" as densely as cells within the upper layer, and thus allow for the presence of voids. Those spaces reflect 50 to 60 percent of the encountered NIR wavelengths (Grind GIS) (SEOS) (Fig. 9). Therefore, by using ratios of red and NIR bands it is possible to isolate vegetation based upon reflectivity.

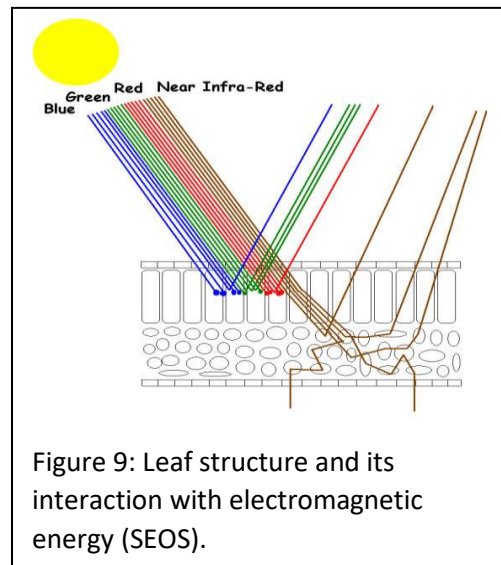


Figure 9: Leaf structure and its interaction with electromagnetic energy (SEOS).

The first attempt to remove vegetation used the Normalized Difference Vegetation Index (NDVI). However, the carbonates within the study area were found to also contain properties that reflected NIR wavelengths higher than expected. That undesirably reduced the difference between vegetation and bedrock reflectance values. Therefore, the Soil Adjusted Vegetation Index (SAVI) was utilized instead. This index was preferable over NDVI because it applies a soil correction factor (Fig. 10). A larger difference between vegetation and bedrock was achieved by setting that correction factor to 0.5.

(NDVI) Formula	(SAVI) Formula
$\frac{(NIR - R)}{(NIR + R)}$	$\frac{(NIR - R)(1 + L)}{(NIR + R + L)}$
R = Red Band, NIR = Near Infrared Band, and L = Soil correction factor (for which a value of 0.5 was used)	

Figure 10: A table defining the functions used for the Normal Difference Vegetation Index (NDVI), and the Soil Adjusted Vegetation Index (SAVI).

A point shapefile was then created to identify a range of reflectance values for vegetation within the study area. ArcMap's Extract Multiple Values to Points tool was used to pull SAVI values at those locations and add them to the attribute table of the shapefile. The minimum and maximum values were identified and used in ArcMap's Set to Null tool. This tool allowed the Researcher to mask out all vegetation that displayed reflectance values within that range from the SAVI layer. Additionally, the identified range of vegetation reflectance values were also used to remove vegetation from the DSM raster, and the thermal layer. To accomplish that the range of vegetation values according were again used. However, in the case of the DSM and the thermal layers, values from the SAVI layer that were desirable were replaced with the values from either the appropriate layer (Fig. 11).

With a majority of large trees and shrubs removed from data, a shapefile containing points at karst sites was then created. To locate those points as accurately as possible, three rasters were used. First, RGB and NIR were used to create a false color composite, in which the red bands were used to display near infrared data, green bands were used to display red wavelengths, and blue bands were used to display green wavelengths. The false color composite was then used in combination with a custom stretch of color bands to gain a better visual of the known karst features. Similarly, a custom stretch was also applied to the TIR imagery. However, in that instance it was done to locate fine differences between the temp. of karst openings and the surrounding area. Finally, the SAVI layer was used to locate karst features by identifying local lows among reflectance values.

While the location decided upon usually matched between the false color composite and the SAVI layers, thermal data sometimes disagreed. The reason for that anomaly is likely the result of thermal plumes, or dissolution features which have collapsed but still allow for air exchange. Once the location of the karst's points were satisfactory, those points were again used as sample sites. Repeating a similar process to that of vegetation removal, the SAVI and TIR rasters were sampled to define a range of values. The Set to Null tool was also again used to filter out values. However, in these instances the identified range of values from sample sites were desirable. Therefore, values from the TIR and SAVI rasters that fell outside of the identified range were set to null (Fig. 12 & 13).

The Digital Terrain Model (DTM), which was created through the removal of vegetation, underwent a smoothing process in which elevation was averaged. To accomplish that, cells that fell within a circle containing a radius of 10 cm took on the average elevation of those cells. This was done because the resolution of the data is so fine that tiny pockets in elevation existed throughout the DTM. Following the smoothing process, the DTM was then used in a hydrological analysis. First the DTM was used to create a flow direction raster. Then, combined with the karst's point shapefile, watersheds were created. The DTM was again used to create a flow accumulation raster. The values of the watersheds were then extracted and used to filter out values from the flow accumulation raster that fell outside identified watershed range (Fig. 14).

These processes resulted in a filtered SAVI layer, a filtered TIR layer, and a filtered flow accumulation layer. ArcMap's Raster Calculator was finally used to identify locations that were common to all three rasters and set all other values to no data (Fig. 15).

Discussion

The results from layering the acquired data provides clear evidence that through limiting an area based on shared characteristics of karst features it is likely possible to identify locations of possible

additional karsting. It is also evident that to successfully reach the goal of mapping karst features through remote sensing, more work is needed. Therefore, possible future work on this study will include identifying additional parameters to limit the area within the results, as well as reexamining parameters that have already been used.

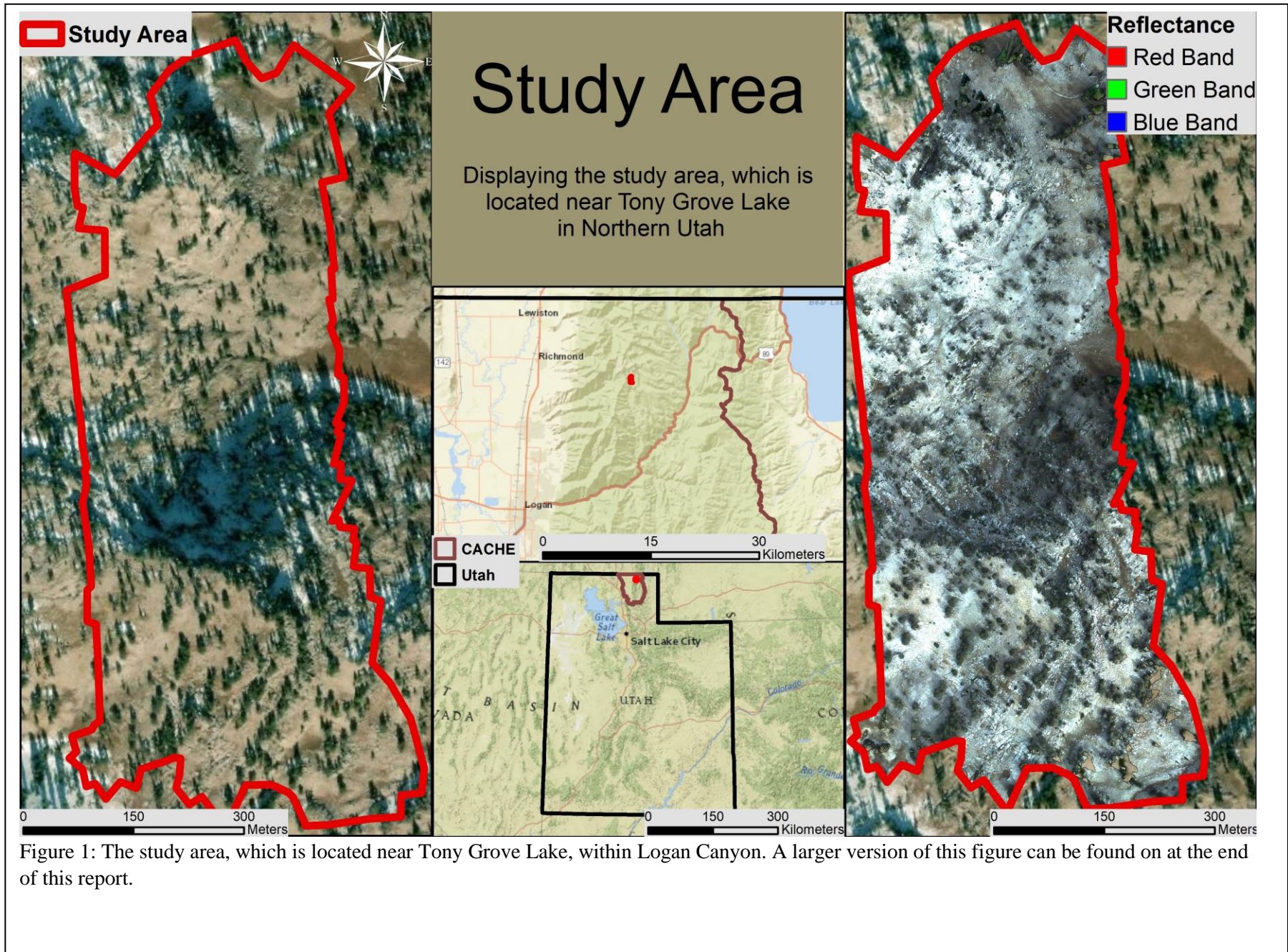


Figure 1: The study area, which is located near Tony Grove Lake, within Logan Canyon. A larger version of this figure can be found on at the end of this report.

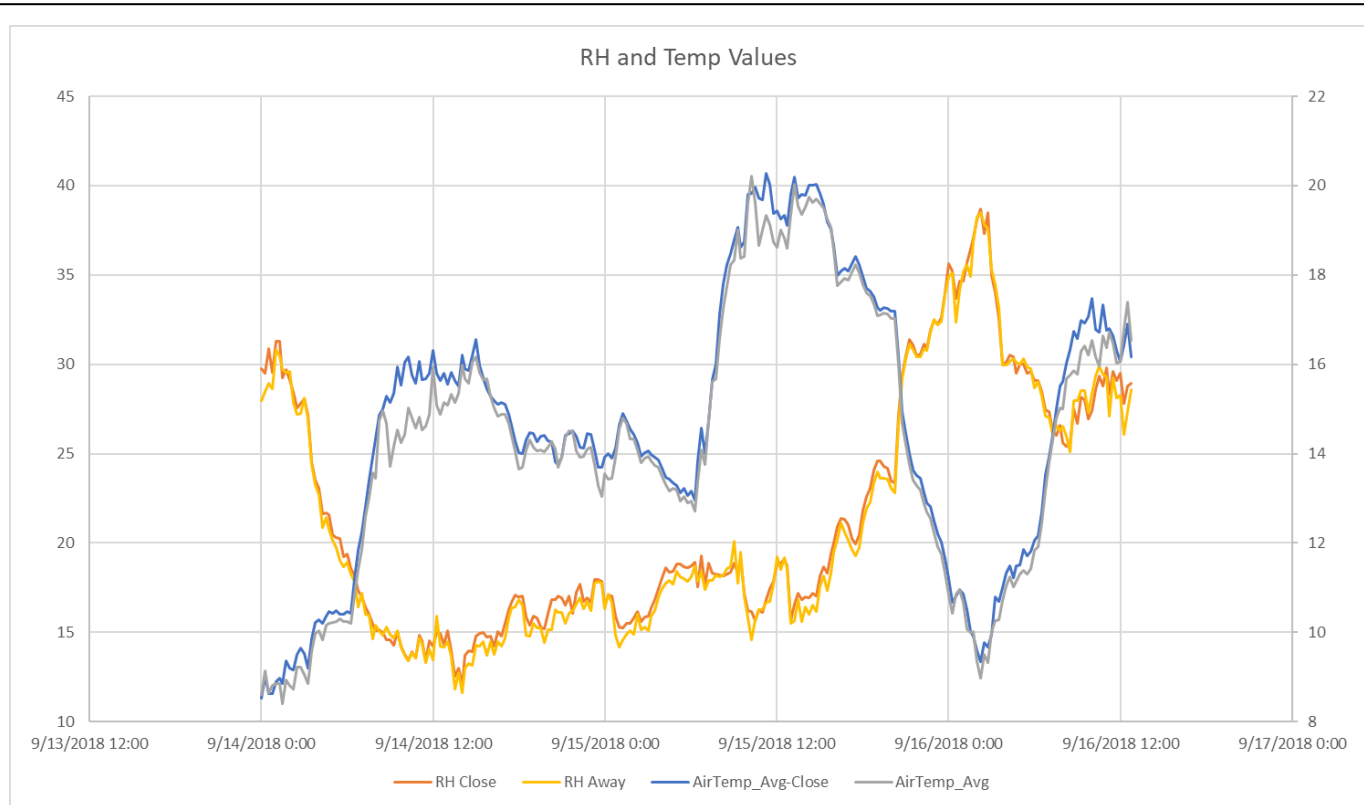


Figure 5: Relative humidity and temperature data for 9/14/18 through 9/16/18. This data shows that the greatest difference in the monitored variables at the monitored karst feature and the surrounding area occurs between 9 AM and Noon. A larger figure is provided at the end of the report.

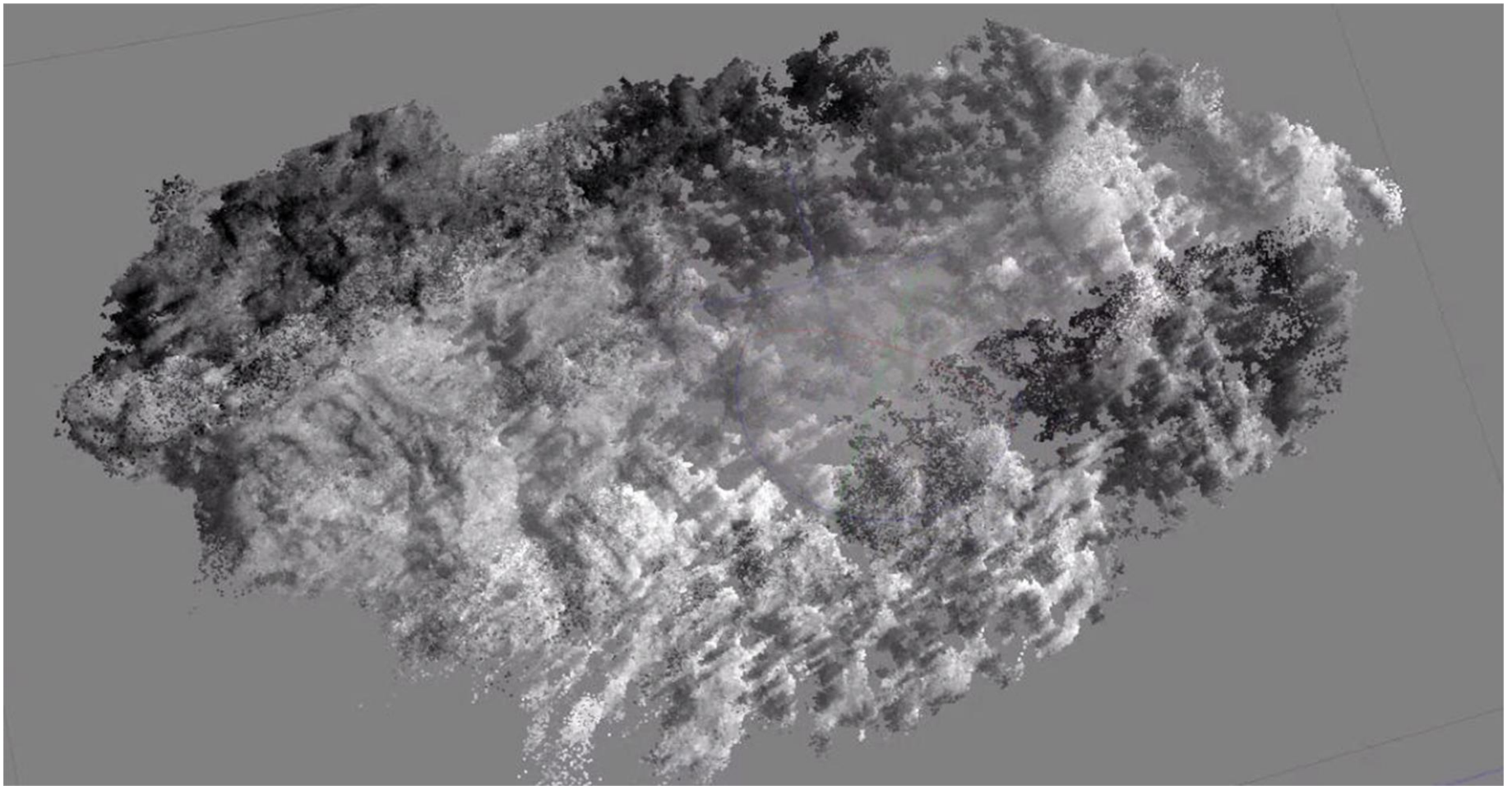


Figure 6: An example of the result of a thermal sensor warming over the duration of a flight path. Notice the beginning of the flight path (top) is dark (cold). Whereas the end of the flight path (bottom) is warmer (lighter).

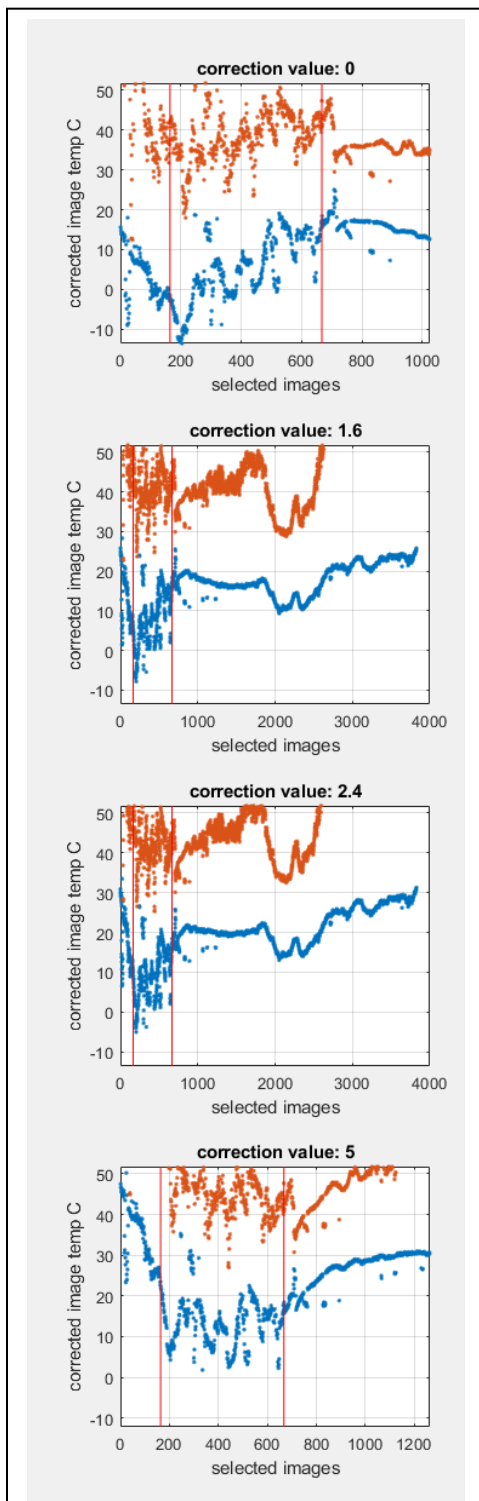


Figure 7: Graphs all plotting the same data from thermal images collected during the aerial survey of the study area. Notice MATLAB's applied correction factors altered the graphs. In the end it was the correction factor of 5 that was used.

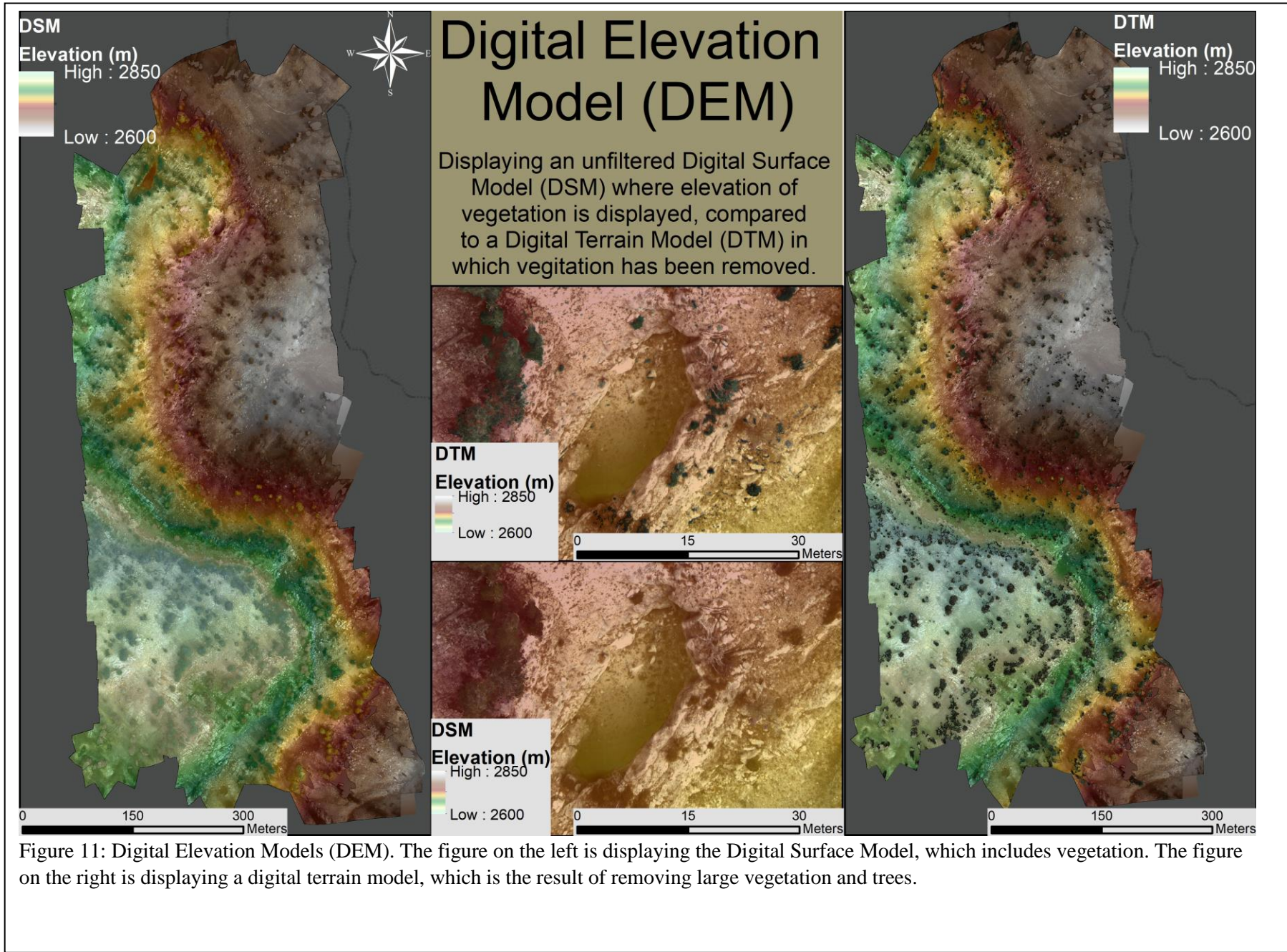


Figure 11: Digital Elevation Models (DEM). The figure on the left is displaying the Digital Surface Model, which includes vegetation. The figure on the right is displaying a digital terrain model, which is the result of removing large vegetation and trees.

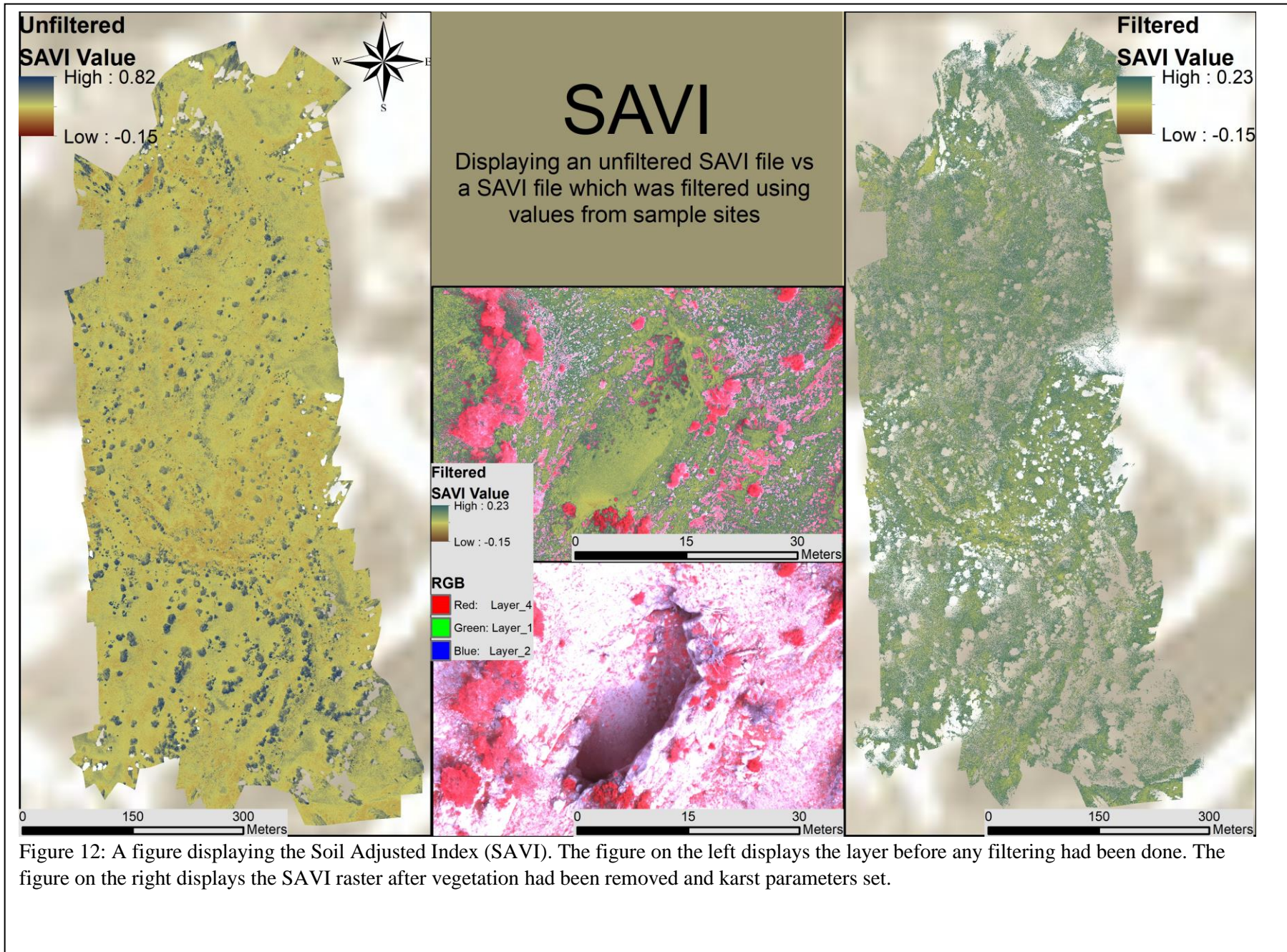


Figure 12: A figure displaying the Soil Adjusted Index (SAVI). The figure on the left displays the layer before any filtering had been done. The figure on the right displays the SAVI raster after vegetation had been removed and karst parameters set.

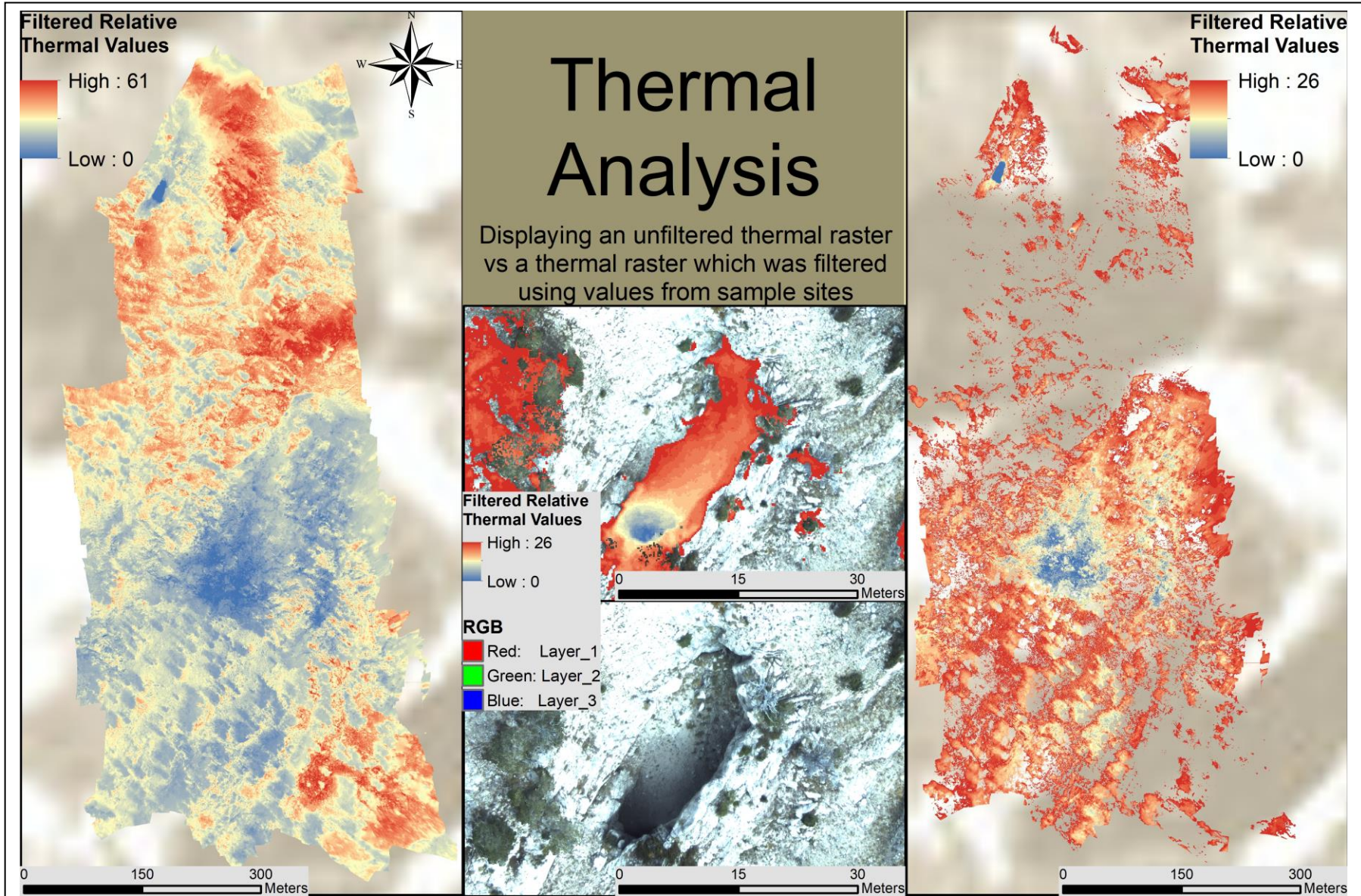


Figure 13: A figure displaying thermal data before any filtering, and after the karst parameters were applied.

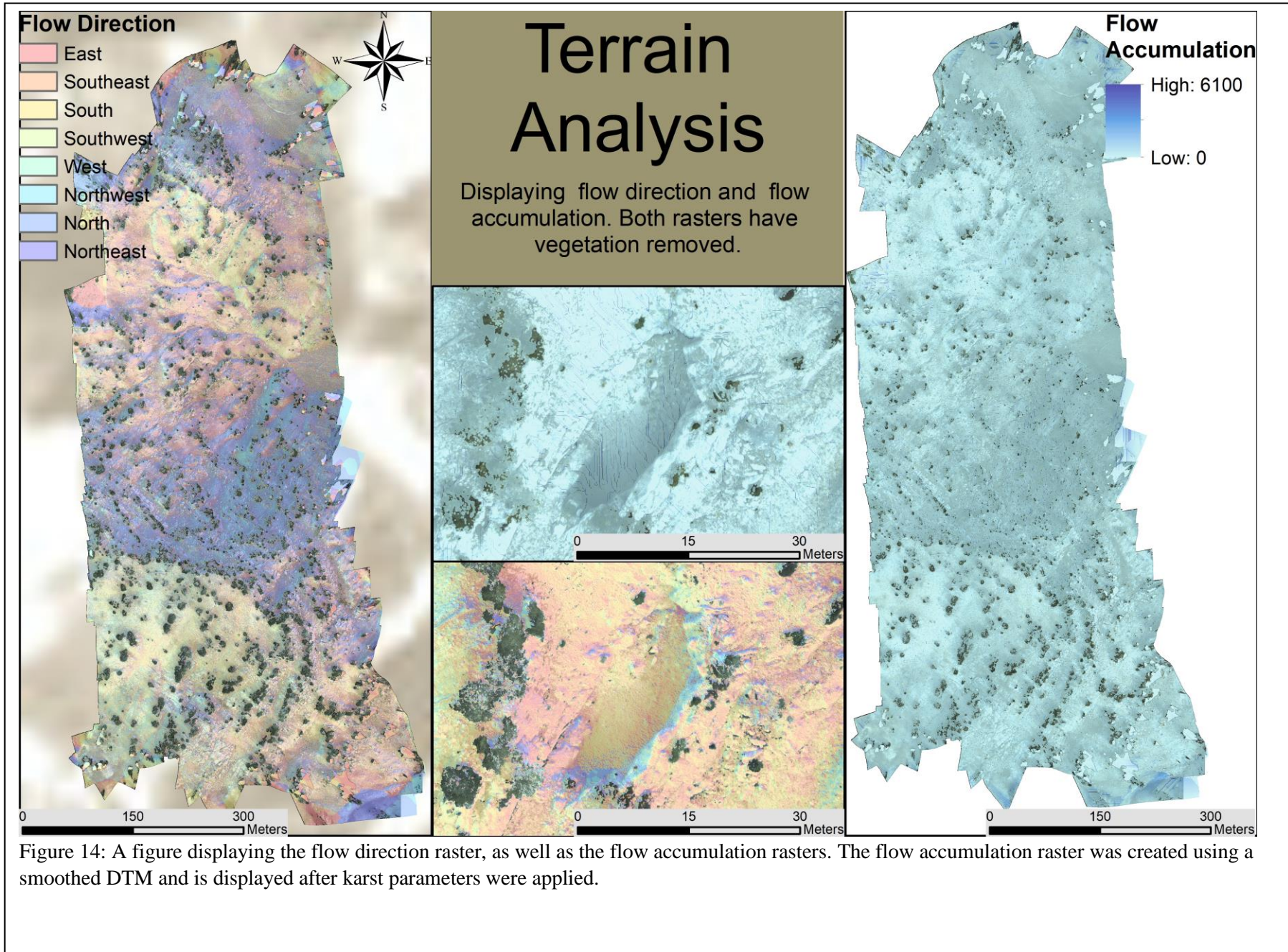
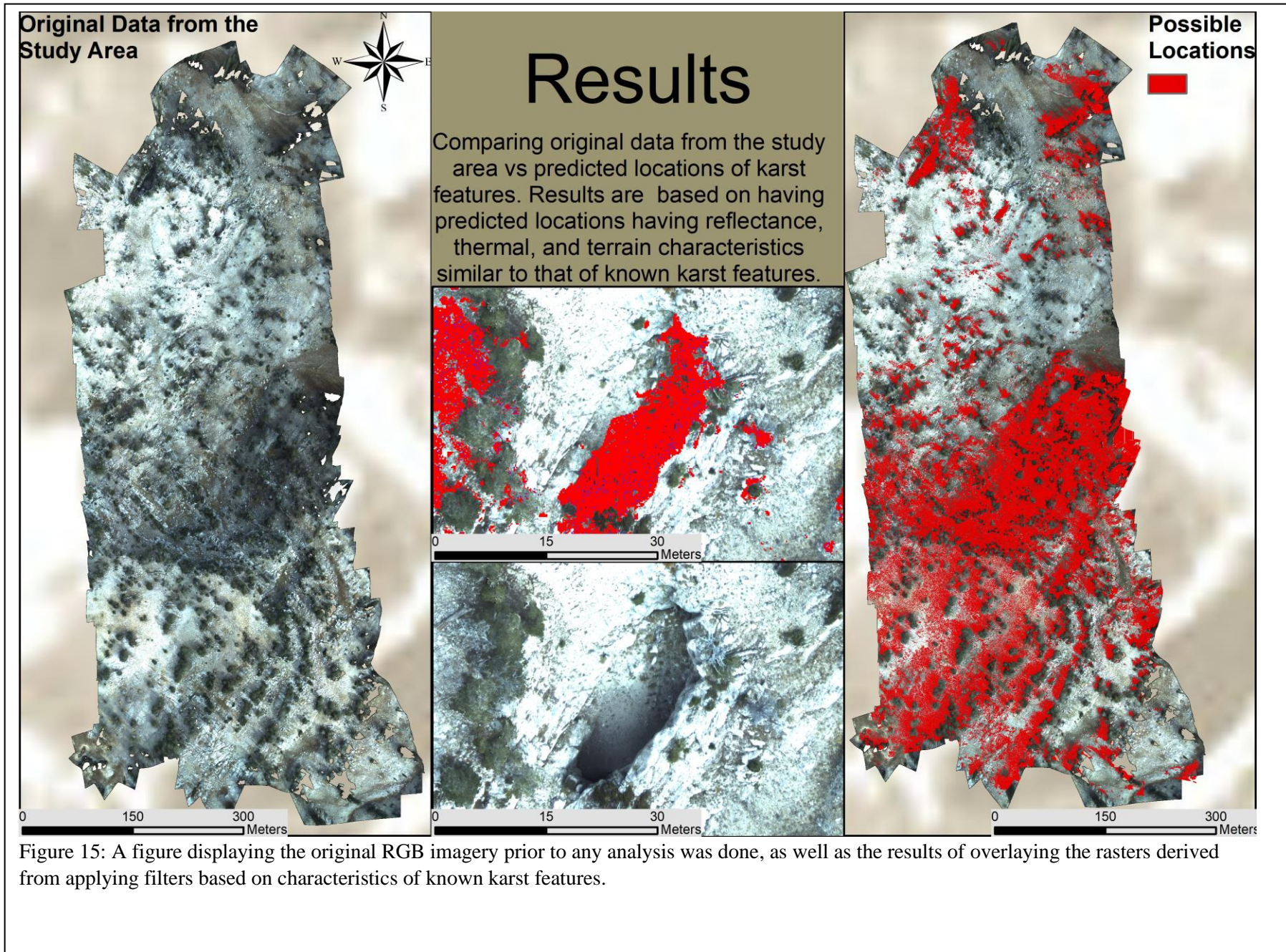


Figure 14: A figure displaying the flow direction raster, as well as the flow accumulation rasters. The flow accumulation raster was created using a smoothed DTM and is displayed after karst parameters were applied.



```
""" Python Script for Final Project """

"""Dane Brophy"""

#Importing modules import arcpy import os import numpy as np import matplotlib.pyplot as plt from
arcpy.sa import * from arcpy import env

#Checking out the spatial extension arcpy.CheckOutExtension('spatial')

#Allowing overwrite arcpy.env.overwriteOutput = True

#Defining path to week 2 data arcpy.env.workspace = r'H:\AAA_Project_Files\Project_Output'

#Defining input for RGB/NIR and TIR inRaster_TIR='20180929_tonygrove_poly2_tir_uncalib_Cel.tif'
inRaster_RGB='20180929_tonygrove_poly2_rgbnir_reflectance.img'
inRaster_DSM='20180929_tonygrove_poly2_rgbnir_DSM.tif' inKarstFeatures = 'Karst.shp'
inVegSampling = 'Vegetation.shp'

#Defining Bands red = arcpy.sa.Raster(inRaster_RGB+'Layer_1') NIR =
arcpy.sa.Raster(inRaster_RGB+'Layer_4')

#*****

#Calculating SAVI

#Defining output file for SAVI out_SAVI_file = 'SAVI.tif'

# delete only if file exists if os.path.exists(out_SAVI_file):  arcpy.delete(out_SAVI_file)

#Assigning a value to the correction factor L=arcpy.sa.Float(0.5)

#Defining SAVI equation SAVI_num = arcpy.sa.Float(NIR - red)*(1 + L) SAVI_denom =
arcpy.sa.Float(NIR + red + L)

# Calculating the SAVI SAVI = arcpy.sa.Divide(SAVI_num, SAVI_denom)

#Saving the SAVI file SAVI.save(out_SAVI_file)

print "SAVI Complete"

#*****

#Extract Multiple Values to Points using vegetation sample points

# Execute ExtractValuesToPoints arcpy.sa.ExtractMultiValuesToPoints(inVegSampling, out_SAVI_file,
"BILINEAR")
```



```
print "Extraction Complete"
#####
#Pulling the values of SAVI from the sampled vegetation shapefile veg_values = [row[0] for row in
arcpy.da.SearchCursor(inVegSampling, 'SAVI')]

#Assigning variables for the max and min of sampled vegetation veg_max=(max(veg_values))
veg_min=(min(veg_values))

print veg_min print veg_max

print "Done sampling vegetation for SAVI values"
#####
#Creating a DTM without vegetation #Values from the SAVI file that are equal to or greater than
lowest sampled #vegetation value get set to null

#Defining output file for DEM out_DEM_file = 'DEM_SAVI.tif'

#Delete only if file exists if os.path.exists(out_DEM_file):  arcpy.delete(out_DEM_file)

# Set local variables inRaster = out_SAVI_file inFalseRaster = inRaster_DSM whereClause = "VALUE >
.35"

# Execute SetNull where values of SAVI which are higher than .35 are set to Null #Other values then
take on the values of the DSM outSetNull = SetNull(inRaster, inFalseRaster, whereClause)

# Save the output outSetNull.save(out_DEM_file)

print "Done removing vegetation"
#####
#Running Focal Statistics tool to smooth the DEM

#Defining output file for DEM out_smooth_DEM_file = 'Focal_SAVI_R5.tif'

#Delete only if file exists if os.path.exists(out_smooth_DEM_file):
arcpy.delete(out_smooth_DEM_file)

#Running Focal Statistics to smooth DEM through an averaging circle of radius 5
arcpy.gp.FocalStatistics_sa(out_DEM_file, out_smooth_DEM_file, "Circle 5 CELL",
"MEAN", "DATA")

print "Done smoothing DEM"
#####
```

```
#Values from the SAVI file that are equal to or greater than lowest sampled #vegetation value get set to null. Other values take on thermal values
```

```
#Defining output file for Thermal with veg removed out_Therm_file = 'Therm_SAVI.tif'
```

```
#Delete only if file exists if os.path.exists(out_Therm_file): arcpy.delete(out_Therm_file)
```

```
# Set local variables inRaster2 = out_SAVI_file inFalseRaster2 = inRaster_TIR whereClause = "VALUE > .35" #whereClause = "VALUE > 'veg_min'"
```

```
# Execute SetNull where values of SAVI which are higher than .35 are set to Null #Other values then take on the values of the Thermal values outSetNull = SetNull(inRaster2, inFalseRaster2, whereClause)
```

```
# Save the output outSetNull.save(out_Therm_file)
```

```
print "Done removing vegetation from thermal file"
```

```
#####
```

```
#Running Focal Statistics tool to smooth the Thermal
```

```
#Defining output file for DEM out_min_Therm_file = 'Therm_SAVI_min_R5.tif'
```

```
#Delete only if file exists if os.path.exists(out_min_Therm_file): arcpy.delete(out_min_Therm_file)
```

```
#Running Focal Statistics to enhance minimum values for thermal over a circle #of radius 5
```

```
arcpy.gp.FocalStatistics_sa(out_Therm_file, out_min_Therm_file, "Circle 5 CELL",
```

```
"MINIMUM", "DATA")
```

```
print "Done enhancing thermal minimum"
```

```
#####
```

```
#Extract Multi Value to Points
```

```
# Set local variables inRasterList = [out_SAVI_file, out_Therm_file]
```

```
# Execute ExtractValuesToPoints arcpy.sa.ExtractMultiValuesToPoints(inKarstFeatures, inRasterList, "BILINEAR")
```

```
print "Extraction Complete"
```

```
#####
```

```
#Pulling values of sampled SAVI from the karst shapefile SAVI_values = [row[0] for row in
```

```
arcpy.da.SearchCursor(inKarstFeatures, 'SAVI')]
```

```
#Assigning variables for the max and min of sampled vegetation SAVI_max=(max(SAVI_values))
```

```
SAVI_min=(min(SAVI_values))
```

```
print 'The minimum sampled SAVI value is', SAVI_min print 'The maximum sampled SAVI value
is',SAVI_max

print "Done sampling karst for SAVI values"
#*****
#Pulling values of sampled SAVI from the karst shapefile Therm_values = [row[0] for row in
arcpy.da.SearchCursor(inKarstFeatures,      'Therm_SAVI')]

#Assigning variables for the max and min of sampled vegetation Therm_max=(max(Therm_values))
Therm_min=(min(Therm_values))

print 'The minimum sampled THERMAL value is', Therm_min print 'The maximum sampled THERMAL
value is', Therm_max

print "Done sampling karst for THERMAL values"
#*****
#Values from the SAVI file that are between the highest and lowest sampled #karst value get set to
null

#Defining output file for DEM out_SAVI_Smple_file = 'SAVI_Samp.tif'

#Delete only if file exists if os.path.exists(out_SAVI_Smple_file):  arcpy.delete(out_SAVI_Smple_file)

# Set local variables inRaster = out_SAVI_file inFalseRaster = out_SAVI_file whereClause = "VALUE >
.23274 & VALUE < .05864"

# Execute SetNull where values of SAVI which are within sampled interval are #set to Null... Other
values then take on the values of the DSM outSetNull = SetNull(inRaster, inFalseRaster, whereClause)

# Save the output outSetNull.save(out_SAVI_Smple_file)

print "Done filtering SAVI"
#*****
#Values from the Thermal file that are between the highest and lowest sampled #karst value get set
to null

#Defining output file for DEM out_Therm_Smple_file = 'Therm_Samp.tif'

#Delete only if file exists if os.path.exists(out_Therm_Smple_file):
arcpy.delete(out_Therm_Smple_file)

# Set local variables
```



```
inRaster = out_Therm_file inFalseRaster = out_Therm_file whereClause = "VALUE > 26.50 & VALUE < 3.79"
```

```
# Execute SetNull where values of Thermal which are within sampled interval are #set to Null... Other values then take on the values of the DSM outSetNull = SetNull(inRaster, inFalseRaster, whereClause)
```

```
# Save the output outSetNull.save(out_Therm_Smple_file)
```

```
print "Done filtering Thermal"
```

```
#####
```

```
#Calculating Flow Direction
```

```
#Calculated Degrees of Slope output file
```

```
Out_Smoothed_FlowDirect=('Flow_Direct_SAVI_Smoothed.tif')
```

```
#Delete only if file exists if os.path.exists(Out_Smoothed_FlowDirect):
```

```
arcpy.delete(Out_Smoothed_FlowDirect)
```

```
#Calculating the flow direction from the DEM and using a flow direction type of D8
```

```
arcpy.gp.FlowDirection_sa(out_smooth_DEM_file, Out_Smoothed_FlowDirect,
```

```
"NORMAL", "", "D8")
```

```
print "Done calculating Flow Direction using smoothed DEM"
```

```
#####
```

```
#Calculating Flow Accumulation
```

```
#Calculated Degrees of Slope output file Out_FlowAccum=('Flow_Accum.tif')
```

```
#Delete only if file exists if os.path.exists(Out_FlowAccum): arcpy.delete(Out_FlowAccum)
```

```
#Calculating the flow Flow Accumulation arcpy.gp.FlowAccumulation_sa(Out_Smoothed_FlowDirect,
```

```
Out_FlowAccum, "", "FLOAT", "D8")
```

```
print "Done calculating Flow Accumulation"
```

```
#####
```

```
#Calculating watersheds of sample sites using the flow direction calculated #from the smoothed flow direction file
```

```
#Calculated Degrees of Slope output file
```

```
Out_SDVI_Watershed=('Watershed_Smoothed_FlwDir_SAVI.tif') ##Delete only if file exists if
```

```
os.path.exists(Out_SDVI_Watershed): arcpy.delete(Out_SDVI_Watershed) ##Running watershed
```

```
tool arcpy.gp.Watershed_sa(Out_Smoothed_FlowDirect, inKarstFeatures,
Out_SDVI_Watershed, "OBJECTID")

print "Watershed complete"
#*****
#Pulling watershed values for the sampled karst locations

Watershed_values = [row[0] for row in arcpy.da.SearchCursor(Out_SDVI_Watershed,
'Count')]

#Assigning variables for the max and min of sampled vegetation
WtrShd_max=(max(Watershed_values)) WtrShd_min=(min(Watershed_values))

print 'The maximum sampled THERMAL value is', WtrShd_max

print "Done sampling karst for Watershed values"
#*****
#Values from the Flow Accumulation file that are equal to or greater than #lowest sampled watershed
value get set to null

#Defining output file for filtered Flow Accumulation out_Filt_FlwAcc_file =
'Filtered_Flow_Accum_Less6100.tif'

#Delete only if file exists if os.path.exists(out_Filt_FlwAcc_file): arcpy.delete(out_Filt_FlwAcc_file)

# Set local variables inRaster = Out_FlowAccum inFalseRaster = Out_FlowAccum whereClause =
"VALUE > 6100"

# Execute SetNull where values of Flow Accumulation which are higher than 6100 #are set to Null.
outSetNull = SetNull(inRaster, inFalseRaster, whereClause)

# Save the output outSetNull.save(out_Filt_FlwAcc_file)

print "Done filtering Flow Accumulation"
#*****
#Using raster calculator to clip the SAVI and Thermal rasters
arcpy.gp.RasterCalculator_sa(("SAVI_Samp.tif" == "Therm_Samp.tif") &
("Therm_Samp.tif" == "SAVI_Samp.tif"), "SAVIThrm_Clip.tif")
#*****
```

```
#Using raster calculator to clip the SAVI and Thermal rasters arcpy.gp.RasterCalculator_sa(  
'("SAVIThrm_Clip.tif" == "Filtered_Flow_Accum_Less6100.tif") &  
("Filtered_Flow_Accum_Less6100.tif" == "SAVIThrm_Clip.tif")', "FlowAccum_Clp.tif")
```


Citations:

- Bahr, K., (2016)"Structural and Lithological Influences on the Tony Grove Alpine Karst System, Bear River Range, North Central Utah". All Graduate Theses and Dissertations. Paper 5015.
- Doerfliger, N., Jeannin, P. -, & Zwahlen, F. (1999). Water vulnerability assessment in karst environments: A new method of defining protection areas using a multi-attribute approach and GIS tools (EPIK method). *Environmental Geology*,39(2), 165-176. doi:10.1007/s002540050446
- Janecke, S.U., and Evans, J.C., 1999, Folded and faulted Salt Lake Formation above the Miocene to Pliocene New Canyon and Clifton detachment faults, Malad and Bannock Ranges Idaho: Field trip guide to the Deep Creek half graben and environs, in Hughes, S.S., and Thackray, G.D., eds., Guidebook to the Geology of Eastern Idaho: Pocatello, Idaho Museum of Natural History, p. 71-96.
- Kresic, N., (2013). *Water in Karst: Management, vulnerability, and restoration*. New York: McGraw-Hill.
- Neilson, B., Tennant, H., Stout, T. L., Miller, M., Gabor, R. S., Jameel, Y., Millington, M., Gelderoos, A., Bowen, G., & Brooks, P. (2018). Stream centric methods for establishing groundwater contributions in karst mountain watersheds. *Water Resources Research*. In review.
- Planet Team (2017). Planet Application Program Interface: In Space for Life on Earth. San Francisco, CA. <https://api.planet.com>
- Spangler, L. (2011). Karst hydrogeology of the Bear River Range in the vicinity of the Logan River, northern Utah. *Geological Society of America Rocky Mountain-Cordilleran Section Meeting*. Retrieved May 17, 2011.
- Sweeney, M. S. (2008). Last unspoiled place: Utah's Logan Canyon. Washington, D.C.: National Geographic.
- Utah Epscor. (n.d.). IUTAH - innovative Urban Transitions and Aridregion Hydro-sustainability. Retrieved March 30, 2018, from <http://iutahepscor.org/>
- Utah State University. "AggieAir." *AggieAir | USU*, Utah Water Research Laboratory, www.aggieair.usu.edu/.
- Williams, S. J. (1948). Geology of the Paleozoic Rocks, Logan Quadrangle, Utah. *Bulletin*; 59 (11): 1121–1164.
- Williams, S. J. (1962). Lake Bonneville: Geology of Southern Cache Valley, Utah. Geological Survey Professional Paper; 257-C